

Integrated Volume Visualisation of Archaeological Ground Penetrating Radar Data

A. Bornik¹ and M. Wallner² and A. Hinterleitner² and G. Verhoeven² and W. Neubauer^{2,3}

¹Ludwig Boltzmann Institute of Clinical-Forensic Imaging, Austria

²Ludwig Boltzmann Institute of Archaeological Prospection and Virtual Archaeology, Austria

³VIAS-Vienna Institute for Archaeological Science, University of Vienna, Austria

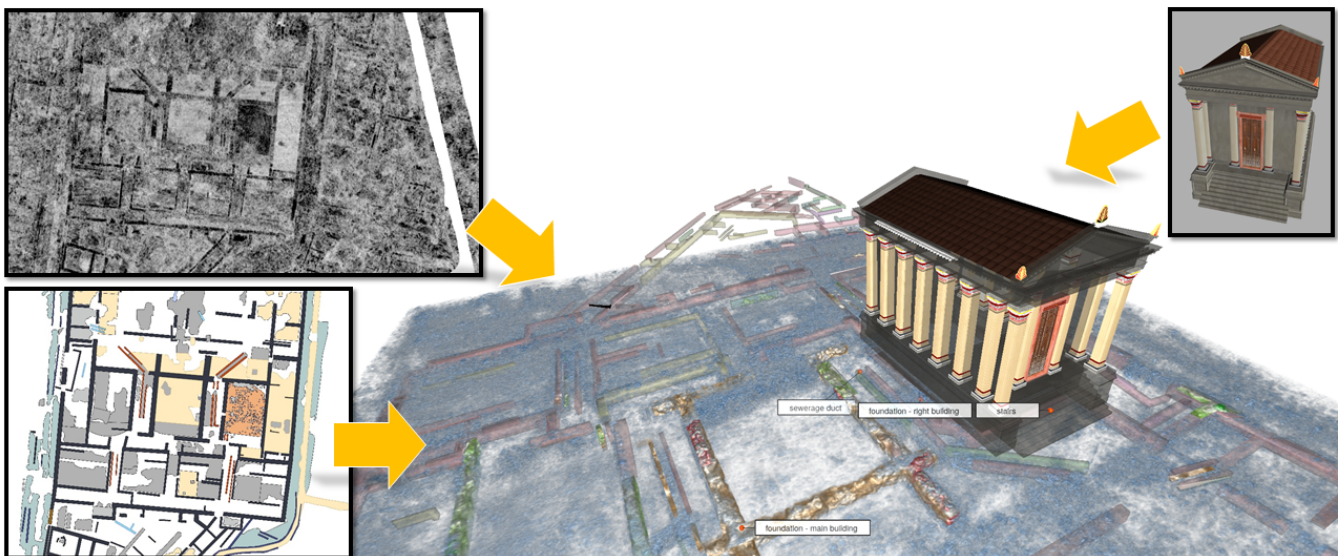


Figure 1: Visualisation of a Roman temple based on GPR data, polyhedral interpretation, reconstructed building and textual annotations.

Abstract

The non-invasive prospection of our archaeological heritage is one of the main tasks of modern archaeology and often provides the necessary bases for further activities, such as special protection or intensified research. Geophysical prospections using ground-penetrating radar (GPR) are an invaluable tool for the non-destructive exploration of archaeological monuments still buried in the ground. However, the analysis and interpretation of the data sets generated in this way is a time-consuming and complex process and requires not only three-dimensional imagination but also a broad understanding of the archaeological remains. Therefore, understandable 3D visualisations are in great demand. This paper presents a novel integrated visualisation approach, which supports conjoint visualisation of scenes composed of heterogeneous data including GPR volumes and 3D models of interpretations and reconstructions. Visual depiction of relevant dataset areas and archaeological structures is facilitated based on flexible and localised visualisation techniques. Furthermore, the rendering system supports the computation of dynamic label layouts for scenes annotations.

CCS Concepts

- Applied computing → Archaeology;
- Human-centered computing → Scientific visualization; Geographic visualization;
- Computing methodologies → Image processing;

1. Introduction

Non-destructive archaeological prospection methods, such as remote sensing, magnetics or ground penetrating radar (GPR), are gaining more and more importance within the archaeological community. Research projects with a focus on the exploration of entire landscapes at places like *Stonehenge*, Carnuntum or the Viking centres of Birka, Kaupang and Borre have pushed the methodological development in recent years [THNea18]. The interpretation of the collected data sets is mostly done manually, although first approaches of a semi-automatic data interpretation have been published [HLea15, PZN15].

The interpretation of GPR data is particular challenging, because of the 3D nature of the data sets. Based on such data, it is possible, for example, to distinguish between a stonewall and the surrounding soil. The primary task of an archaeological interpretation is therefore to identify archaeologically significant structures, to graphically define and interpret them in an archaeological way. Despite its 3D nature, archaeologists often analyse GPR by browsing through the individual 2D slices of the datasets, which is similar to the way how radiologists read CT or MRI datasets. However, unlike in radiology where physicians try to identify deviations from known healthy anatomy, the three-dimensional structures in archaeological GPR data are unknown. Archaeologists need to develop a thorough understanding of their composition and shape. This clearly demands 3D visualisation of the data at hand and 3D tools for expert interpretation. The presented method of a joint visualisation of manually interpreted GPR data and calculated 3D volumes represents a revolutionary way to the understanding of this complex geophysical prospection method. For the first time it is possible to generate an optimised representation of the archaeological structures still hidden in the ground through a two-way adaptation of manual interpretation and calculated visualisation. This provides an exceptional basis for further analyses and simulations. The possibility to integrate 3D models, e.g. from virtual archaeology modelling, further aids the dissemination of the scientific results through comprehensible virtual representations.

2. Related work

High resolution GPR data for archaeological prospection are computed from the reflections of an emitted electromagnetic pulse by the subsoil recorded using a measuring point interval of around 4x4 cm. The intensity of the reflections depends on the geophysical properties of the structures lying in the ground. The recorded GPR waves are band-pass filtered and migrated and the absolute amplitude of the wave is calculated in the time domain corresponding to the depth range of the 3D data cube, here 5cm [NEHSM02, Con04].

For archaeological interpretation, the GPR datasets are visualised as accumulated grey scale images for arbitrary depth ranges or as video clips of the 5 cm depth range. Dark image regions indicate strong reflections by walls or stone structures. (see Fig. 2).

GIS tools are frequently used to integrate and visualise GPR datasets, since the support globally referenced positioning and flexible integration of any type of data in form of overlays [Arc]. However, support for 3D datasets is limited. Software used in radiology offers direct volume rendering based on a global mapping from

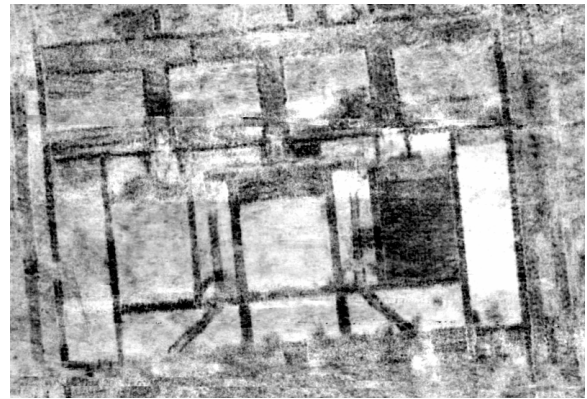


Figure 2: Grey scale image representing the depth range between 1.0 m and 2.0 m of a GPR dataset.

dataset values to color and transparency (transfer functions), but neither offers support for non-volumetric data nor functionality for local control of the visualisation style [RSEH*06]. Other tools, like *Voxler* or *VG Studio* are more flexible. However their functionality to locally control the visualisation outcome, to integrate non-volumetric datasets are limited [Vox, Vol].

3. Methods

This paper presents an integrated solution for visualisation of archaeological GPR datasets, their interpretation and reconstructed 3D models.

3.1. Data preprocessing

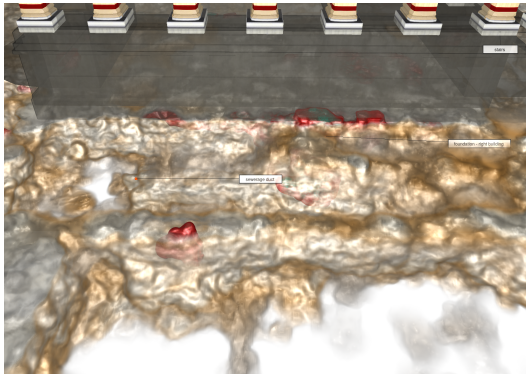
The noise level in GPR datasets is typically high. In addition, dataset values for small structures like stones strongly differ from the ones representing intermediate layers like mortar. Direct visualisation shows all the details in the data, but fails to isolate meaningful large scale structures. Contiguous visualisations of, e.g. building foundations, require a higher degree of dataset homogeneity, which is facilitated using on state-of-the-art denoising algorithms, which remove high frequency noise while edges of large structures are preserved. Dataset filtering is performed on the GPU alongside visualisation. Filter parameters can be adjusted at any time to meet the visualisation goal [ULP14, ROF92].

3.2. Visualisation

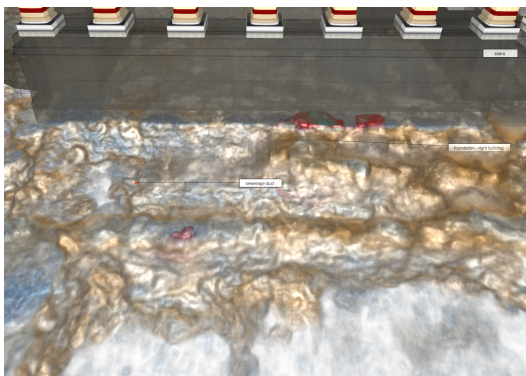
The proposed visualisation system is based on a hybrid volume and surface data rendering algorithm inspired by [KGB*09]. 3D models like virtual reconstructions and the bounding cubes of the interpreted GPR datasets are rendered to a HA-buffer [LHL13], which results in a memory efficient representation of sorted fragments lists for each pixel. Each fragment stores an object ID in addition to colour and transparency. In a second rendering pass, these lists are traversed maintaining a set of active objects. Front-facing fragments indicate objects being entered, back facing exited ones. Colour/transparency values from the current fragment are

combined with the results from volume ray casting all active GPR objects until the next fragment is reached. Ray segment results are blended in front-to-back order.

Sampling multiple filtered and unfiltered versions of the dataset using different transfer functions allows to visually combine multiple features of the dataset (see Fig. 3).



(a)



(b)

Figure 3: Combined volume/surface visualisation based on TV-L1 filtered GPR dataset and a semi-transparent reconstructed 3D model (a). Integration of a second unfiltered GPR dataset for fine-grained detail information (b).

3.2.1. Local visualisation control

The archaeological interpretation is typically available as a series of polygons manually drawn on individual dataset slices. 3D models for visualisation are obtained through slice extrapolation and fusion. Fig. 4 shows an example of conjoint visualisation of interpretation data (building foundations and sewerage ducts) and the underlying dataset.

A more flexible way of data overlay is achieved utilising the active object set information. This approach inspired by work in [BUSea18] allows to exclude regions inside or outside a particular 2-manifold 3D model from ray casting or to select different transfer functions and/or versions of the datasets per ray segment/fragment interval. In archaeology this functionality can be used to visually

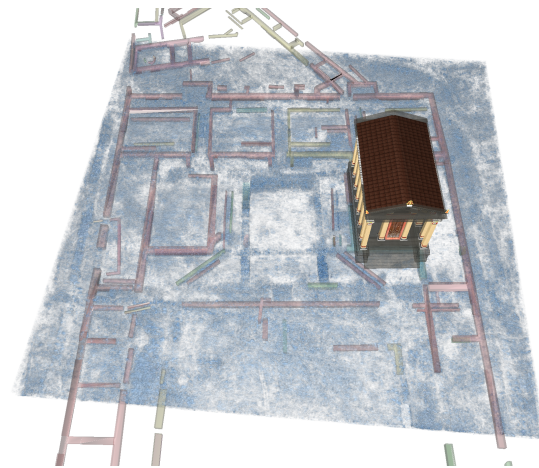


Figure 4: Overlay of unfiltered GPR dataset, polyhedral interpretation and reconstructed 3D model.

depict dataset portions enclosed by manually generated interpretation objects (see Figs. 5(a) and 1) based on real data rather than the comparably coarse interpretation mesh.

3.3. Dataset annotation

Self-explanatory archaeological illustrations require textual annotations of important structures. The proposed approach features an automated dynamic label placement solution inspired by [SKSB17], which decouples dataset annotation, which only needs to be done once, and per frame layout computation. To account for the semi-transparent nature of the scenes at hand, labels are placed outside, on top of and inside the model.

4. Experiments and Results

The here presented example shows a not yet excavated part of the Roman forum of Carnuntum, which is one of the largest building complexes within the former civil town [Neu14]. Remains of Roman stone walls, steps, floors and sewerage canals are clearly recognisable in the GPR data recorded using a motorised 16-channel ground penetrating radar (MIRA) with an antenna frequency of 400MHz. The resulting dataset counts 4096x4096x52 voxels at a resolution of 10x10x4 cm [THNea18]. The interpretations dataset used consist of more than 800 individual objects counting around 15k vertices and 10k triangles in total.

The dataset was filtered using the TV-L1 denoising algorithm with $\lambda = 1.15$ to reduce the noise level for GPR visualisation outside the two selected objects from the interpretation and $\lambda = 0.5$ to visualise the two wall segments. Furthermore, four annotations were placed. Rendering times on a NVidia GTX 1080 GPU for a frame buffer size of 1920x1080 are interactive, ranging from around 50 (perpendicular to ground plane) to 150 ms (parallel). In the latter case the higher depth complexity and the larger number of volume samples per ray were found to be the major impact factors.

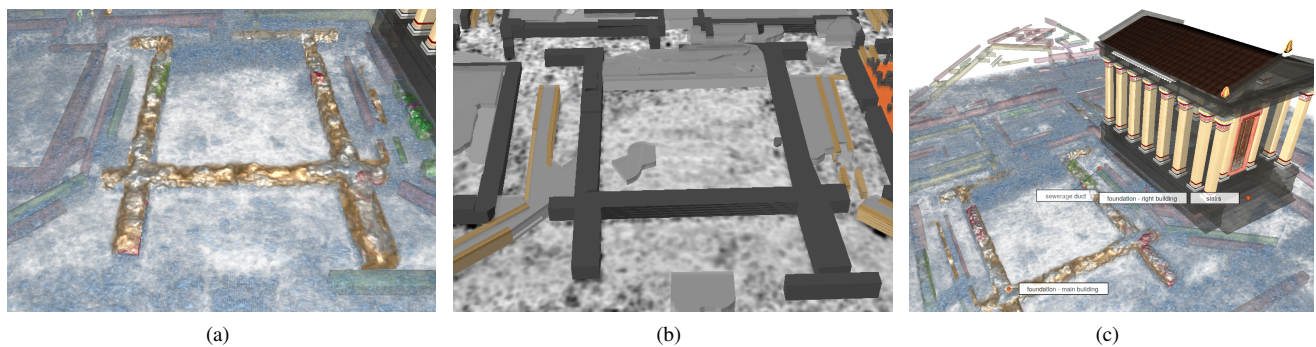


Figure 5: Visualisation of interpretation objects in full 3D GPR dataset based on two differently filtered copies. The application domains of three different transfer functions for foundation walls A and B (orange and green) and the background (blue) are determined based on the 3D geometry of the respective 3D meshes (a). Conventional state-of-the-art visualisation of complete archaeological interpretation of a GPR dataset based on 2,5D model and a single (2D) GPR slice (b). View of the same scenario using the proposed visualisation techniques showing the complete GPR dataset, geometric and volumetric interpretation representations, and annotations (c).

5. Discussion & Future Work

The experiments carried out so far have clearly shown the potential of the proposed approach. Archaeologists were impressed by its fidelity (Fig. 5(a) and 5(c)) over the state-of-the-art (Fig. 5(b)) and by the possibilities to evaluate interpretations elaborated on a slice by slice basis comparing them to the 3D data evidence in the respective regions. Our first investigations revealed numerous interpretation inaccuracies and inconsistencies, which can be related to the limitations of 2D views of 3D data. Future work will therefore address 3D visualisation support in the data analysis and interpretation phase. The suitability of interactive segmentation techniques from medical image analysis will be investigated.

6. Acknowledgements

The geophysical survey was conducted by the Ludwig Boltzmann Institute for Archaeological Prospection and Virtual Archaeology (LBI ArchPro) in cooperation with the Central Institute for Meteorology and Geodynamics (ZAMG) as part of the research project *ArchPro Carnuntum* funded by the Amt der Niederösterreichischen Landesregierung. The reconstructed 3D model was provided by Michael Klein, 7reasons.

References

- [Arc] About ArcGIS - the mapping and analytics platform. URL: <https://www.esri.com/en-us/arcgis/about-arcgis/overview>. 2
- [BUSea18] BORNİK A., URSCHLER M., SCHMALSTIEG D., ET AL.: Integrated computer-aided forensic case analysis, presentation, and documentation based on multimodal 3d data. *Forensic Science International* 287 (2018), 12–24. 3
- [Con04] CONYERS L. B.: *Ground-Penetrating Radar for Archaeology*. AltaMira Press, Walnut Creek, CA, 2004. 2
- [HLea15] HINTERLEITNER A., LÖCKER K., ET AL.: Automatic detection, outlining and classification of magnetic anomalies in large-scale archaeological magnetic prospection data. In *Archaeological prospection. 11th Intl. Conf.* (2015), Rzeszotarska-Nowakiewicz A., (Ed.), Polish Academy of Sciences, pp. 296–299. 2
- [KGB*09] KAINZ B., GRABNER M., BORNİK A., HAUSWIESNER S., MUEHL J., SCHMALSTIEG D.: Ray casting of multiple volumetric datasets with polyhedral boundaries on manycore gpus. *ACM Trans. Graph.* 28, 5 (2009), 152:1–152:9. 2
- [LHL13] LEFEBVRE S., HORNUS S., LASRAM A.: *HA-Buffer: Coherent Hashing for single-pass A-buffer*. Research Report RR-8282, INRIA, apr 2013. 2
- [NEHSM02] NEUBAUER W., EDER-HINTERLEITNER A., SEREN S., MELICHAR P.: Georadar in the roman civil town carnuntum, austria: an approach for archaeological interpretation of gpr data. *Archaeological Prospection* 9, 3 (2002), 135–156. doi:10.1002/arp.183. 2
- [Neu14] NEUBAUER W.: Die Entdeckung des Forums der Zivilstadt. In *Carnuntum. Wiedergeborene Stadt der Kaiser*, Humer F., (Ed.) von Zabern, 2014. 3
- [PZN15] POSCETTI V., ZOTTI G., NEUBAUER W.: Improving the GIS-based 3D mapping of archeological features in GPR data. In *Archaeological prospection. 11th Intl. Conf.* (2015), Rzeszotarska-Nowakiewicz A., (Ed.), Polish Academy of Sciences, pp. 603–607. 2
- [ROF92] RUDIN L. I., OSHER S., FATEMI E.: Nonlinear total variation based noise removal algorithms. *Physica D: Nonlinear Phenomena* 60, 1-4 (1992), 259–268. 2
- [RSEH*06] REZK-SALAMA C., ENGEL K., HADWIGER M., KNISS J. M., WEISKOPF D.: *Real-time Volume Graphics*. Taylor & Francis Ltd., 2006. 2
- [SKSB17] SIRK C., KALKOFEN D., SCHMALSTIEG D., BORNİK A.: Dynamic Label Placement for Forensic Case Visualization. In *EuroVis 2017 - Short Papers* (2017), Kozlikova B., Schreck T., Wischgoll T., (Eds.), The Eurographics Association. doi:10.2312/eurovisshort.20171147. 3
- [THNea18] TRINKS I., HINTERLEITNER A., NEUBAUER W., ET AL.: Large-area high-resolution ground-penetrating radar measurements for archaeological prospection. *Archaeological Prospection*, May (2018), 1–25. doi:10.1002/arp.1599. 2, 3
- [ULP14] URSCHLER M., LEITINGER G., POCK T.: Interactive 2d/3d image denoising and segmentation tool for medical applications. In *Proceedings MICCAI Workshop Interactive Medical Image Computation (IMIC)* (2014). 2
- [Vol] VG Studio Max - Die High-End-Software für industrielle CT. URL: <https://www.volumegraphics.com/de/produkte/vgstudio-max.html>. 2
- [Vox] Voxler - power forward into 3d visualization. URL: <http://www.goldensoftware.com/products/voxler>. 2